Determination of chiral indices of individual single- and double-walled boron nitride nanotubes by electron diffraction

R. Arenal[a)]
Materials Science Division, Argonne National Laboratory, Illinois 60439

M. Kociak
Laboratoire de Physique Solides, CNRS-Université Paris-Sud, 91405 Orsay, France

A. Loiseau
Laboratoire d'Etude des Microstructures, ONERA-CNRS, 92322 Châtillon, France

D.-J. Miller
Materials Science Division, Argonne National Laboratory, Illinois 60439

(Received 22 March 2006; accepted 30 June 2006; published online 15 August 2006)

The intensities of electron diffraction patterns from individual (single-, double-walled) boron nitride nanotubes (BNNTs) as well as from bundles of these tubes have been recorded. The helicities have been systematically measured, and the diameter and the chiral indices have been determined. The analysis of 121 nanotubes reveals that 12% of the tubes are zigzag, while the distribution of the other helicities is uniform. The large value of the intertube distance and the significant difference of the chiral angle between the two constituent tubes in double-walled BNNTs indicate a lower interaction between the BN sheets than in bulk hexagonal BN. © *2006 American Institute of Physics*. [DOI: 10.1063/1.2335379]

Boron nitride nanotubes (BNNTs) show an insulating character with a constant band gap ($\geqslant$5.5 eV) independent of their helicity and diameters.[1,2] This leads to interesting optical properties of these inorganic tubes, which make them a possible alternative to their carbon nanotube (CNT) counterparts with regard to possible applications. Nevertheless, in contrast to CNTs for which many studies have shown their atomic structure, this information is still needed for BNNTs despite the fact that this is a key to understanding their growth mechanism.

BNNTs and CNTs share the same structure, with the difference of replacing a C–C pair with a B–N pair. Their structure can be described by a set of two chiral indices (n,m), or equivalently a diameter (d) and a helicity (ϕ).[3] However, most of the techniques used for determining diameters and helicity in CNT are not compatible with BNNT because they do not apply to wide band gap nanostructures (e.g., Raman[4] or scanning tunneling microscopy[5]). Transmission electron microscopy (TEM), either in high resolution (HRTEM) or electron diffraction (ED), does not suffer from this constraint. While HRTEM has been used to measure diameters, and in few cases chiral angles, ED is now routinely used to obtain reliable measurements of the chiral indices of CNTs.[3,6–8] Together with the fact that a theory for simulating the ED patterns (EDPs) of a BNNT already exists,[9] ED is an important technique for measurement of chiral indices.

Regarding the helicity of BNNTs, several studies were carried out using HRTEM and ED. Our HRTEM work on single-walled BNNTs (SWBNNTs) revealed that the configuration of the tubes is mainly zigzag.[10,11] This configuration was also shown in HRTEM on multiwalled BNNTs (MWBNNTs) obtained by different synthesis processes (see Ref. 12, for example). With regard to the ED approach, Golberg *et al.*[13] concluded that their MWBNNTs are mainly zigzag. In contrast, two other groups[14,15] found that their investigated MWBNNTs did not show a dominant helicity. However, none of the previous studies ever determined chiral indices. Further, EDPs of model systems such as SWBNNTs, ropes of SWBNNTs, and double-walled BNNTs are not yet acquired.

In this letter, we present the first ED study of individual SWBNNTs and double-walled BNNTs (DWBNNTs), as well as ropes of SWBNNTs. Chiral angles of all of these nanotubes and the diameters of 26 of them have been measured. From this information, together with comparison with theory, the chiral indices of almost all of these tubes have been determined.

BNNTs were grown using a continuous laser vaporization technique.[10,11,16] This technique is actually the only one that provides SWBNNTs. Using this process, the tubes are mainly SW, with some (20%) MW (primarily double walled). They are either isolated or organized in small bundles (two to ten tubes).

Since an individual BNNT is usually separated from another tube or nanoparticle by less than a few tens of nanometers, a small and parallel illuminating probe is required for ED from a single tube. This was obtained in a Tecnai F20 transmission electron microscope equipped with a field emission gun operated at 100 keV using the nanoprobe mode with the smallest condenser aperture. In this mode, the image of the condenser aperture is projected over the sample, providing a highly coherent and parallel nanometer-scale ($\sim$50 nm) electron beam. The ED patterns were recorded using a Gatan Ultrascan charge-coupled device camera, with no blooming effect observed. The average acquisition time was only 8 s, and we could usually acquire several EDP without damaging the tubes.

In the following, we will describe the EDPs of SWNT and DWNT, and the analysis method to extract chiral indices

[a)]Electronic mail: arenal@anl.gov

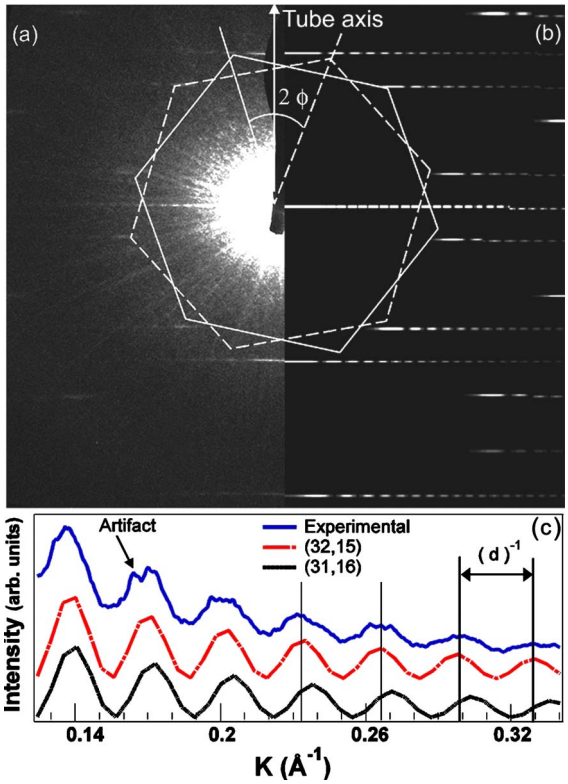

FIG. 1. (Color online) (a) Experimental and (b) simulated EDPs of a SWBNNT. (c) Intensity profiles of the Eq-L of the experimental and simulated EDPs of this tube. The tube was tilted at an angle of 20° from the incident beam direction. This inclination was taken into account in the simulated EDP.

based on two representative examples. A short description of EDP analysis of ropes will follow. Figures 1(a) and 1(b) show the experimental and simulated EDPs (see below), respectively, of a SWBNNT. It is important to note that the EDP from a BNNT is very similar to that obtained from a CNT (see, e.g., Refs. 6, 7, and 17), as Lambin and Lucas predicted.[9] In a heuristic model, a SWNT is considered as two parallel BN sheets rotated with respect to each other by 2ϕ; thus the EDPs are the superposition of two rotated trigonal networks. This explains why the first intensity maxima in a SWNT roughly form two hexagons (Fig. 1). For further analysis, it is more interesting to consider that the intensity is discretely distributed on lines (so-called layer lines[9]) perpendicular to the direction of the tube axis, oscillating in the perpendicular direction.[3,9] The central line is referred to as the equatorial line (Eq-L). As Gao *et al.*[7] showed, the helicity of a nanotube is easily deduced by measuring the ratio of the layer line distances. The tube diameter can be extracted from the period of pseudo-oscillations along the layers. In practice, we measured the period spacing on the last oscillations of the Eq-L. For the SWNT in Fig. 1, the helicity is $18.37° \pm 0.19°$ and its diameter is 3.27 ± 0.06 nm. Based on these values, and including the experimental errors, a set of possible chiral indices can be deduced.[6] In this example, there are two possibilities: (31,16) and (32,15). In almost all cases, the ambiguity can be eliminated by comparison with simulation using the DIFFRACT program (see Refs. 6 and 9). For instance, comparing the profiles of the Eq-L extracted from the experimental and simulated EDPs [see Fig. 1(c)] shows unambiguously that the solution is (32,15).

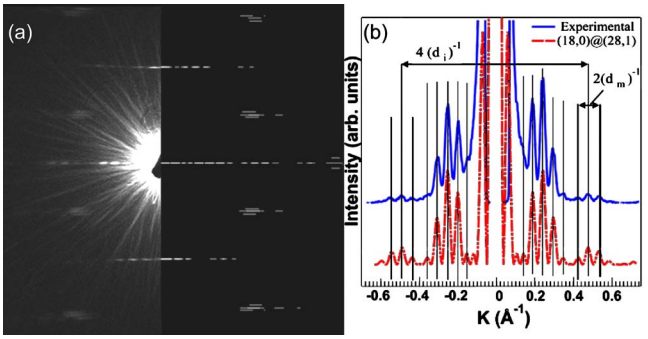

FIG. 2. (Color online) (a) Experimental EDP of a DWBNNT (left) and simulated pattern (right). (b) Intensity profiles of the Eq-L of the experimental and simulated EDPs of this tube.

Except for the equatorial line, on which contributions of the two constituting shells interfere, the EDP of a DW NT can be interpreted as the simple superposition of the layer lines of the two constituting tubes. Once each set of layer lines has been attributed to a given shell using the heuristic model describing the EDP of each nanotube as two triangular networks as a guide (see Ref. 6), the helicities of each shell can be extracted as described previously for SWNT. Because the Eq-L oscillates with two frequencies equal to the mean diameter (d_m) and the intertube distance[6] (d_i) (see Fig. 2), diameters can be measured directly on the EDP. Figure 2 shows the image and EDP of a DWBNNT. Chiral angles are $0.0° \pm 0.02°$ and $1.96° \pm 0.08°$, respectively, and d_m and d_i have values of 1.85 ± 0.09 nm and 0.41 ± 0.02 nm, respectively. With this level of error, we usually retrieved a single set of chiral indices for DWNTs directly. However, we always confirmed our results with fits to theoretical results as described in Ref. 6. In this case, the DWNT was found to be (18,0)@(28,1).

Concerning the analysis of DWBNNTs, we note that the interlayer distance measured in these NTs, between 0.38 and 0.42 nm, is much larger than the interlayer distance in *h*-BN [0.33 nm (Ref. 11)]. A similar behavior has been observed in DWCNTs also[18] and it could be seen as a *collective effect*: when the number of layers becomes large the global interaction between them is higher than in the case of a few sheets. For DWBNNTs this value of interlayer spacing is larger (almost 10%) than for DWCNTs.[18] These larger values are likely due to the heteroatomic nature of BN because a repulsion could exist between the atoms of boron (or N) in one of the networks and those in the other layer. As for the DWCNT, we observed that this interspacing distance enhancement is not dependent on the curvature of the tubes. In addition, we did not observe any correlation of the chiral angle between the constituent nanotubes in the concentric DWNTs: for 66% of the DW tubes investigated, the difference in helicities of the two independent tubes is larger than 7°. This is in contrast to large MWBNNTs (composed of more than 30 walls) where, as Ref. 15 found, there is an interlayer correlation. Our results on DWBNNTs indicate a lower interaction between the BN sheets in this configuration than in the case of bulk *h*-BN or MWBNNTs with a large number of walls.

Helicities of ropes comprised of a small number of SWNT have also been measured, thanks to the fact that, as for the DWNT, EDPs of a rope are identical to the superposition of its constituent SWNT. The analysis of the Eq-L is

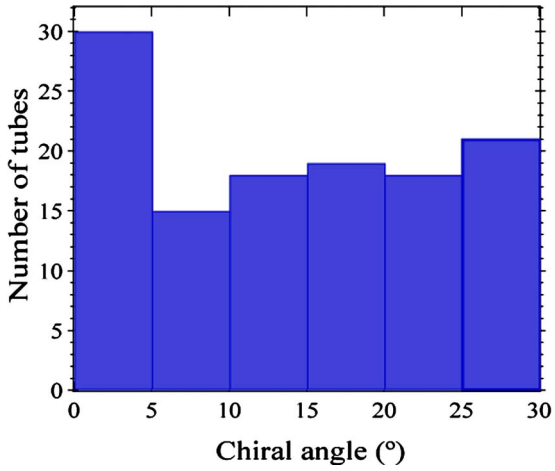

FIG. 3. (Color online) Number of tubes as a function of the chiral angle.

not as straightforward and is now under consideration.

We now turn to the analysis of the helicities. We acquired the EDP of 7 SW-, 23 MW BNNTs (21 DW), and 26 ropes (mostly containing only two tubes). Chiral angles have been deduced for all tubes, and diameters for all SW and 19 DW tubes were also determined. In addition, we obtained the chiral indices for most of the SW and DW nanotubes. Figure 3 shows the distribution of the helicity of the tubes. In this compilation, each tube forming a MWBNNT and a bundle is considered an independent NT. Thus, the total number of tubes studied is 121. 25% of tubes have helicities between 0° and 5°, among which 12% are strictly zigzag. Excluding the latter, we note that the distribution is roughly uniform. On the other hand, we only found 3% strictly armchair tubes. These results are consistent with our results with HRTEM.[10,11] Using first-principles molecular dynamics simulations, Blase *et al.*[19] showed that the growth of zigzag BNNTs requires the existence of a catalyst particle. Our phenomenological formation model[11,16] is based in a root-growth mechanism where boron nanoparticles act as growth precursors. Thus, the formation of the nanotube results from the reaction between a drop of boron produced by the decomposition of the boron compounds of the target and the nitrogen atoms from the gas flowing in the reactor and from the decomposition of the *h*-BN target. Theoretical findings from Ref. 19 suggest that the strong tendency for the zigzag configuration is due to the role of the boron droplet in the nanotube formation.

We have presented the electron diffraction patterns recorded from a series of SW, DW, and bundles of BNNTs. We have not observed any difference between the EDP of a BNNT and that of a carbon nanotube (see, e.g., Refs. 6, 7, and 17). The analysis of the ED data revealed that 12% of the tubes are zigzag, while the distribution of the other helicities is uniform. This distribution is likely related to the growth of the tubes. This conclusion is in good agreement with our previous TEM studies[10,11,16] and the theoretical work of Ref. 19. Furthermore, we observed that for the double-walled BNNTs, the interlayer distance is larger than that of *h*-BN and that there is no strong correlation between the chiral angles of the two constituent concentric tubes. These differences indicate a lower interaction between the layers for the DWBNNTs than that for *h*-BN or MWBNNTs with a larger number of walls.

This work was supported by the U.S. Department of Energy, Office of Science, under Contract No. W-31-109-ENG-38 and was carried out in the Electron Microscopy Center at Argonne National Laboratory. This work has been done within the framework of the GDRE "NanoE" (No. 2756) of the CNRS. The authors acknowledge helpful discussions with N. J. Zaluzec and R. E. Cook.

[1] X. Blase, A. Rubio, S. G. Louie, and M. L. Cohen, Europhys. Lett. **28**, 335 (1994).
[2] R. Arenal, O. Stephan, M. Kociak, D. Taverna, A. Loiseau, and C. Colliex, Phys. Rev. Lett. **95**, 127601 (2005).
[3] L.-C. Qin, in *Progress in TEM 2, Applications in Materials Science*, Springer Series in Surface Sciences Vol. 39, edited by X. F. Zhang and Z. Zhang (Springer, Berlin, 2001), pp. 73–104.
[4] R. Arenal, A. C. Ferrari, S. Reich, L. Wirtz, J.-Y. Mevellec, S. Lefrant, A. Rubio, and A. Loiseau, Nano Lett. **6**, 1812 (2006).
[5] M. Ishigami, S. Aloni, and A. Zettl, AIP Conf. Proc. **685**, 389 (2003).
[6] M. Kociak, K. Hirahara, K. Suenaga, and S. Iijima, Eur. Phys. J. B **32**, 405 (2003).
[7] M. Gao, J. M. Zuo, R. Twesten, and I. Petrov, Appl. Phys. Lett. **82**, 2703 (2003).
[8] J. C. Meyer, M. Paillet, G. S. Duesberg, and S. Roth, Ultramicroscopy **106**, 176 (2006).
[9] P. Lambin and A. Lucas, Phys. Rev. B **56**, 3571 (1997).
[10] R. S. Lee, J. Gavillet, M. Lamy de la Chapelle, A. Loiseau, J.-L. Cochon, D. Pigache, J. Thibault, and F. Willaime, Phys. Rev. B **64**, 121405(R) (2001).
[11] R. Arenal, Ph.D. thesis, University of Paris XI, 2005.
[12] B. G. Demczyck, J. Cumings, A. Zettl, and R. O. Ritchie, Appl. Phys. Lett. **78**, 2772 (2001).
[13] D. Golberg, Y. Bando, K. Kurashima, and T. Sato, Solid State Commun. **116**, 1 (2000).
[14] T. Laude and Y. Matsui, Eur. Phys. J. B **283**, 293 (2004).
[15] A. Celik-Atkas, J. M. Zuo, J. F. Stubbins, C. Tang, and Y. Bando, Appl. Phys. Lett. **86**, 133110 (2005).
[16] R. Arenal, O. Stephan, J.-L. Cochon, and A. Loiseau (unpublished).
[17] Z. Liu, Q. Zhang, and L.-C. Qin, Phys. Rev. B **71**, 245413 (2005).
[18] K. Hirahara, M. Kociak, S. Bandow, T. Nakahira, K. Itoh, Y. Saito, and S. Iijima, Phys. Rev. B **73**, 195420 (2006).
[19] X. Blase, A. De Vita, J. C. Charlier, and R. Car, Phys. Rev. Lett. **80**, 1666 (1998).